

Measurement of neuropeptide Y with molecularly imprinted polypyrrole on carbon fiber microelectrodes

Luis López ^a, Kelly Lozano ^b, John Cruz ^a, Krystal Flores ^b, Lauren Fernández-Vega ^b, Lisandro Cunci ^{a,*}

^a Department of Chemistry, University of Puerto Rico – Rio Piedras, 17 Ave Universidad Ste 1701, San Juan, PR 00931, United States

^b Department of Chemistry, Universidad Ana G. Méndez, Carr. 189, Km 3.3, Gurabo, PR 00778, United States

ARTICLE INFO

Keywords:
Neuropeptide Y
Molecular imprinting
Biosensor
Carbon fiber microelectrode

ABSTRACT

The measurement of neuropeptides using small electrodes for high spatial resolution would provide us with localized information on the release of neuromolecules. The release of Neuropeptide Y (NPY) is related to different neurological diseases such as stress, obesity, and PTSD, among others. In this conference paper, we electrodeposited polypyrrole on carbon fiber microelectrodes in the presence of NPY to develop a molecularly imprinted polypyrrole sensitive to NPY. Optimization of the electrodeposition process resulted in the full coverage of the polymer with nucleation sites on the carbon fiber ridges, achieving completion by the seventh cycle. Electrodeposition was performed for five cycles, and using cyclic voltammetry (CV), we studied the change in the oxidation current peak for polypyrrole due to the presence of NPY. We also observed a change in capacitance due to the presence of NPY, which was studied by electrochemical impedance spectroscopy (EIS). A linear correlation was found between the oxidation peak and the concentration of NPY between 50 ng/mL and 1000 ng/mL. In addition, a linear correlation was also found between microelectrode capacitance and the concentration of NPY between 50 ng/mL and 1000 ng/mL at 100 kHz.

1. Introduction

Neuropeptides are related to many processes of human life, from hormones that carry chemical signals into the endocrine system to neurochemical messengers that work similarly to small neurotransmitters. (Duvall et al., 2019) NPY is the most abundant neuropeptide in the brain and has been related to diseases such as hypertension, obesity, schizophrenia, (Morosawa et al., 2017) fear, (Tasan et al., 2016) addiction, (Gilpin, 2012) stress, (Wagner et al., 2016) depression, pain, cancer, (Tilan and Kitlinska, 2016) memory, (Götzsche and Woldbye, 2016) and sleep disorders, among others. (Crespi, 2011; Kalra et al., 1990; Langley et al., 2022; Sajdyk, 2005) Currently, there is a lack of an analytical technique that directly measures NPY levels, preventing researchers from understanding the natural role of NPY in these diseases. Each microenvironment under study requires the precise measurement of the different molecules present at appropriate rates depending on the kinetics of each process. (Eugster et al., 2022) Developing analytical techniques has brought the understanding of brain chemistry in space and time, especially electrochemical techniques. Fast scan cyclic

voltammetry (FSCV) and amperometry allowed the researchers to study sub-second processes related to oxidizable molecules (electroactive molecules). (Bath et al., 2000) In the last decade, enzymatic electrodes have been developed using these two techniques to measure non-electroactive molecules. For example, glucose oxidase has been used to measure glucose thanks to the formation of hydrogen peroxide, which is electroactive and can be measured by amperometry. (Lugo-Morales et al., 2013) Researchers have now measured the classic neurotransmitters, which are electroactive molecules. Neuropeptides are classified as non-electroactive molecules for which no method is available. Due to their structural differences compared to classic neurotransmitters, the enzymatic method does not work for detecting neuropeptides because it would require different oxidases for each neuropeptide. The lack of an analytical technique to measure neuropeptides with high temporal and spatial resolution has made the rapid progression in this area difficult.

Neuropeptides are constituted by short amino acid chains synthesized in the soma and dendrites. These peptides are stored in large, dense core vesicles until their release from nerve endings and dendrites. Unlike small neurotransmitters, some neuropeptides do not undergo recycling,

* Corresponding author.

E-mail address: lisandro.cunci@upr.edu (L. Cunci).

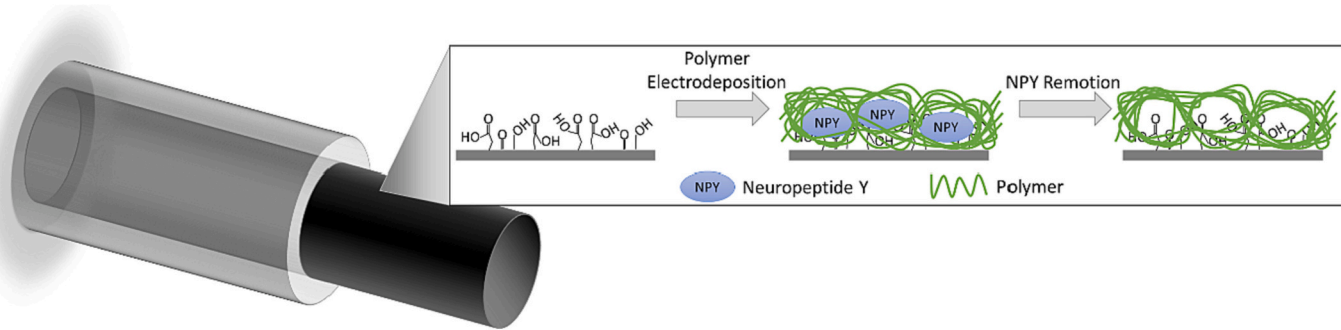


Fig. 1. Molecularly imprinted polypyrrole biosensor fabrication.

lack a reuptake system, and are broken down by peptidases. This demands that the cell synthesize new molecules, sending them from the soma to the nerve endings and dendrites for replacement. Since other small neurotransmitters are typically released alongside neuropeptides, it becomes crucial to devise a highly selective technique for their detection and formulate a strategy to mitigate the signal interference from other neurotransmitters. Electrochemical biosensors (EB) offer a variety of platforms for performing measurements. EB are tools that help transduce biological processes into a quantitative measurement that we can analyze and constantly evolve to achieve higher sensitivity, selectivity, and stability. (Singh et al., 2021) Different strategies are used to measure molecules selectively, such as aptamers, antibodies, enzymes, and molecular imprinting polymers (MIPs). MIPs are materials that can be electropolymerized on the surface of the electrodes with recognition capabilities for specific molecules. They are created by polymerizing functional monomers around a template molecule, resulting in cavities with sizes, shapes, and functionalities complementary to the template. (Yücebas et al., 2020) After template removal, these cavities act as highly selective binding sites for the target molecule, allowing its recognition from a complex mixture. (Ayankojo et al., 2022) MIPs offer several advantages over traditional detection techniques. Their high selectivity minimizes interference from other molecules, while their robust synthetic nature enables modifying their properties for specific applications. Additionally, MIPs can be easily scaled and immobilized on various supports (Feier et al., 2019), making them ideal for sensor development.

In a recent development, J. M. Seibold and colleagues introduced an innovative approach utilizing aptamer-modified microelectrodes for the dynamic measurement of NPY, showcasing promising potential for exceptional spatial and temporal resolution. (Seibold et al., 2023) The researchers achieved precise measurements of NPY in serum. However, it's noteworthy that the microelectrodes used are too big for brain-related analyses, ca. 4 mm in diameter. In a related breakthrough, N. K. M. Churcher and collaborators demonstrated a remarkable detection limit for NPY in sweat, reaching 10 pg/mL (Mintah Churcher et al., 2020) and 50 pg/mL (Churcher et al., 2022) using antibodies and larger electrodes. While this marks substantial progress in the field, a primary challenge persists in the inherent limitations of antibodies, which lack long-term stability. Additionally, the large size of these electrodes poses a hindrance, rendering them unsuitable for utilization in brain-related studies. Our group reported the measurement of NPY concentrations in an implantable platinum microelectrode in concentrations as low as 10 ng/mL in aCSF using aptamers. (López et al., 2021) While we tested biofouling and compared it to carbon fiber microelectrodes, metal microelectrodes still have biofouling problems that are expected to be reduced by depositing polymers on the surface. (Sun et al., 2021; Zhang et al., 2015).

In this conference paper, we use a biosensing method based on molecularly imprinted polymers (MIP) to measure the concentration of Neuropeptide Y (NPY) using carbon fiber microelectrodes. In order to test this technique, NPY₁₋₃₆ has been used in all experiments. Two

techniques were used: CV, which showed a decrease in the current in the presence of NPY, and EIS, we were able to observe a change in the capacitance of the microelectrode due to NPY concentration changes.

2. Methods

2.1. Carbon fiber microelectrodes

In this study, carbon fiber microelectrodes with an approximate diameter of 7 μm were fabricated. These electrodes were sealed using a borosilicate glass capillary (1.0 mm \times 0.5 mm) through a micropipette puller. A single T-hornet T-300 carbon fiber was drawn into the glass capillary using a vacuum pump. The exposed carbon fiber was then cut, and microscopic examination with water immersion ensured a proper seal between the glass and the carbon fiber to prevent solution leakage into the capillary, thereby preserving the electroactive area. An electrical connection was established using silver paint and a silver-plated copper wire. The fiber was cut using a razor blade, producing a uniform and reproducible bare carbon fiber electrode surface. The carbon fiber length was ca. 150 μm . Finally, the electrodes were soaked in isopropanol and subjected to ultrasonic cleaning to remove debris from their surfaces.

2.2. Physical characterization

Scanning electron microscopy (SEM) coupled was used to obtain the changes in the composition of the surface of the electrodes after fabrication. An SEM-EDS model, JSM-6010LA from JEOL, was used.

2.3. Reagents

Electrochemical characterization of carbon-fiber microelectrodes was carried out in artificial cerebrospinal fluid (aCSF) at pH 7.4 prepared with 150 mM NaCl, 1.4 mM CaCl₂, 3 mM KCl, 0.8 mM MgCl₂, 0.8 mM Na₂HPO₄·7H₂O, 0.17 mM NaH₂PO₄·2H₂O, 0.5 M Tris in nanopure water 18.2 MΩ. Neuropeptide Y (GenScript) was diluted in aCSF to prepare the standard solutions. The volume of the electrochemical cell used was 15 mL. The electrochemical cell was stirred for 1 min after adding NPY aliquots and waited until the solution was steady to avoid convection effects.

2.4. Electrochemical synthesis of molecularly imprinted polypyrrole-based microelectrodes

Electrochemical synthesis of modified carbon-fiber microelectrodes MIPs was prepared by electropolymerization of pyrrole on the carbon-fiber microelectrode using CV from -0.4 to 0.8 V at 100 mV/s for five cycles. The cell contained 0.5 M pyrrole, aCSF pH 7.4, and 10 $\mu\text{g/mL}$ NPY. The template molecules of NPY were then removed by immersing the MIPpy carbon-fiber microelectrodes in 95% ethanol and DI water for 15 min. The left imprinted PPY/carbon-fiber microelectrodes now

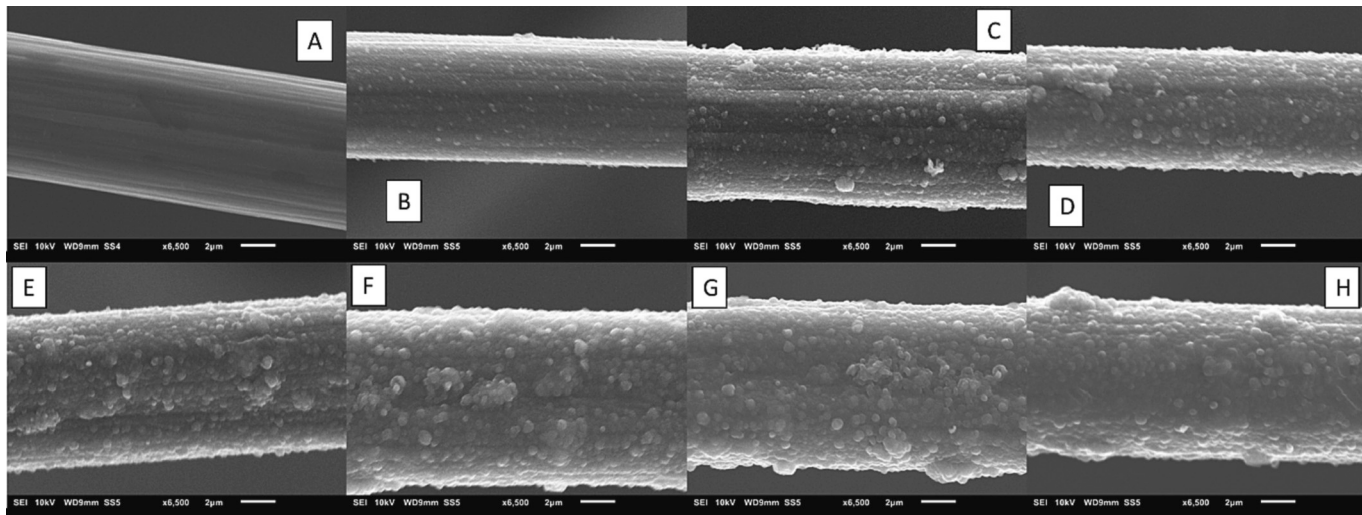


Fig. 2. Scanning electron microscope of carbon fiber microelectrodes (A) before and after being coated with (B) 1, (C) 2, (D) 3, (E) 4, (F) 5, (G) 6, and (H) 7 single electrodepositions of polypyrrole.

contain complementary cavities to interact with NPY for electrochemical measurements.

2.5. Electrochemical measurements

All electrochemical measurements were done using a three-electrode electrochemical cell with the electrodeposited carbon fiber microelectrodes as the working electrode, a platinum wire as the counter electrode, and an Ag|AgCl reference electrode (3 M KCl-filled solution). A Reference 600+ Gamry potentiostat was used for electrochemical measurements, and all data were collected using Gamry Instruments Framework software. All potentials in this work are expressed versus Ag|AgCl. An amplitude of 10 mV, an initial frequency of 100 kHz, and a final frequency of 10 Hz were used for EIS. Data analysis was done using Gamry Echem and OriginPro software.

3. Results and discussion

3.1. Molecularly imprinted polymer electrodeposition

Fig. 1 shows the fabrication of the electrodeposition of molecularly

imprinted polypyrrole (MIPpy) on carbon fiber microelectrodes to detect NPY. Carbon fiber microelectrodes of 150 μ m in length and 7 μ m in diameter were used to electrodeposit polypyrrole. Because most of the electrodepositions tended to break, exposing the carbon fiber surface, we first optimized the electrodeposition of polypyrrole to ensure complete coverage.

SEM can be used to identify the presence of polymers within a surface material. SEM generates high-resolution images showcasing the surface topography. Fig. 2 shows SEM images of carbon fiber microelectrodes in which polypyrrole was electrodeposited. Different techniques can be used to electrodeposit conductive polymers on electrodes, with the typical methods being CV and amperometry. Because of the cyclic nature of CV, it allows good control over the deposition on the surface. Therefore, as shown before, we used CV from -0.4 V to 0.8 V vs. Ag|AgCl as the best limits for the electrodeposition of polypyrrole on carbon electrodes. (Kim et al., 2016; Ping et al., 2022) Fig. 2A shows the carbon fiber microelectrode before electrodeposition with the typical as-drawn Thornel T-300 carbon fiber surface with the regular ridges. Due to the high surface energy of the defects on the carbon fiber surface, electrodeposited polymers are expected to start nucleation at these ridges. After each electrodeposition using CV, we obtained SEM images

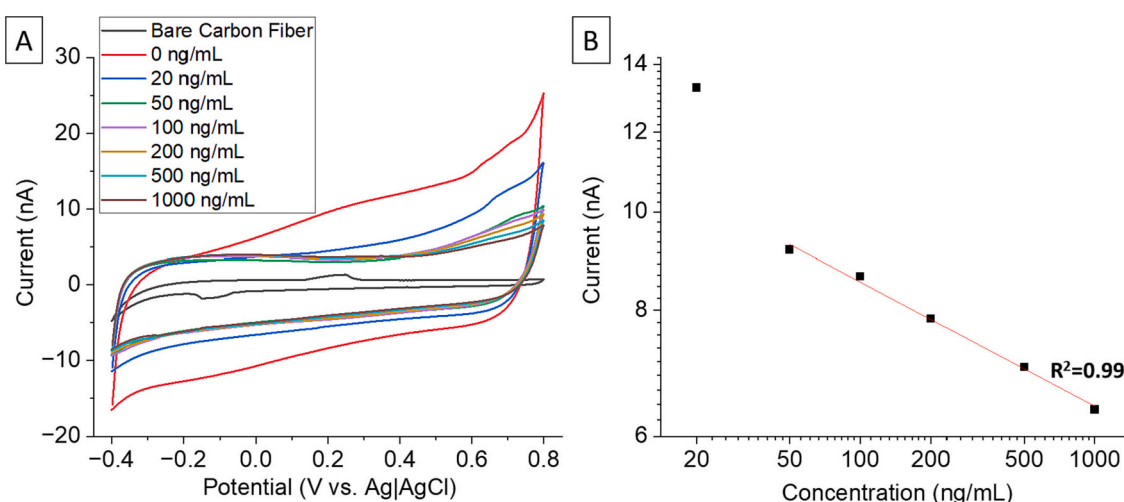


Fig. 3. Cyclic voltammetry of bare carbon fiber microelectrode, as deposited molecularly imprinted polypyrrole (0 ng/mL), and at different concentrations of NPY. (B) The correlation between peak current at 0.73 V and concentration of NPY shows a linear relationship with $R^2 = 0.99$. All measurements were made at 100 mV/s in aCSF at pH 7.4 with all potentials measured against Ag|AgCl electrode.

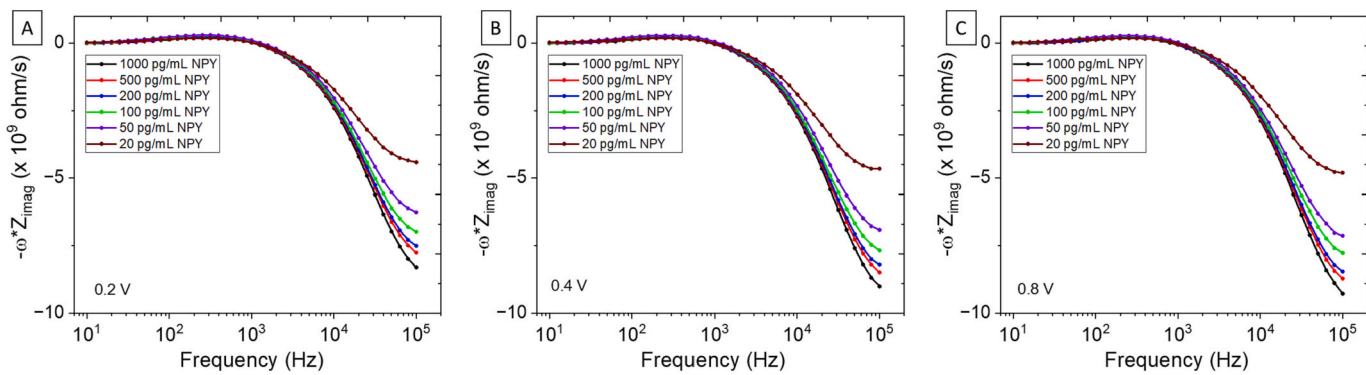


Fig. 4. Background-subtracted electrochemical impedance spectroscopy ($-\omega^*Z_{\text{imag}}$) measured at (A) 0.2 V, (B) 0.4 V, and (C) 0.8 V vs. Ag|AgCl at different concentrations of NPY in aCSF.

to characterize the surface of the carbon fiber microelectrodes to optimize the complete coverage of the electrodes. Each image in Fig. 2B to H shows the same microelectrode with single electrodepositions added. The optimization of this electrodeposition clearly shows the conductive polymer layer forming and covering the carbon fiber microelectrode surface. Figs. S1 to S8 show SEM images of the entire fiber and close-ups of the tip of the fiber to show more detail of the morphology of the deposition. In Fig. 2B, the nucleation sites are distinctly visible along the ridges of the carbon fiber microelectrode. As the polypyrrole electrodeposition progresses, the longitudinal ridges become even more pronounced.

After analyzing images of several electrodes, we found that the coverage of the carbon fiber microelectrode was complete after the fifth electrodeposition (Fig. 2F and Fig. S6). Therefore, the MIPPy with NPY on the carbon fiber microelectrodes was done using five electrodepositions.

CV serves as a tool for biosensing by harnessing the unique electrochemical properties of biomolecules. This technique involves applying a continuously varying voltage to a working electrode. Fig. 3A (black line) shows the CV of bare carbon fiber microelectrode on aCSF at 100 mV/s. Only two peaks can be seen, corresponding to the hydroquinone/quinone redox reaction in oxidized carbon electrodes. (Dekanski et al., 2001) As the MIPPy is deposited and the NPY is removed, the electrode shows the typical CV of polypyrrole, as seen in Fig. 2A (red line). (Rosas-Laverde et al., 2020; Sharma et al., 2010)

3.2. Neuropeptide Y measurement

In order to measure NPY using molecularly imprinted carbon fiber microelectrode, we used two strategies: (1) CV and (2) EIS. When employing a CV to measure the concentration of NPY in polypyrrole, we observed that the oxidation peaks of the polypyrrole deposited on the surface of the microelectrode are influenced by the presence of NPY in the molecularly imprinted sites. By electrodepositing polypyrrole in the presence of NPY and then removing it, we are creating specific molecular sites where NPY interacts with higher affinity compared to non-specific sites, as is typical through common intermolecular forces. By injecting NPY into the solution, it is expected to bind in these sites faster and stronger while preventing the polymer from interacting with the solution and decreasing the oxidation current of the microelectrode. This effect is seen in the oxidation peak of polypyrrole at 0.73 V vs Ag|AgCl. We observed a decrease in the oxidation peak of polypyrrole as the concentration of NPY increases, covering part of the MIP and preventing its oxidation.

Fig. 3A shows the CV obtained at 100 mV/s in the presence of NPY in concentration between 0 ng/mL (as deposited MIPPy) to 1000 ng/mL with a clear decrease in the oxidation peaks of polypyrrole as well as a slight change in the capacitance of the microelectrode seen by increasing the width of the CV. Fig. 3B shows the correlation between the oxidation

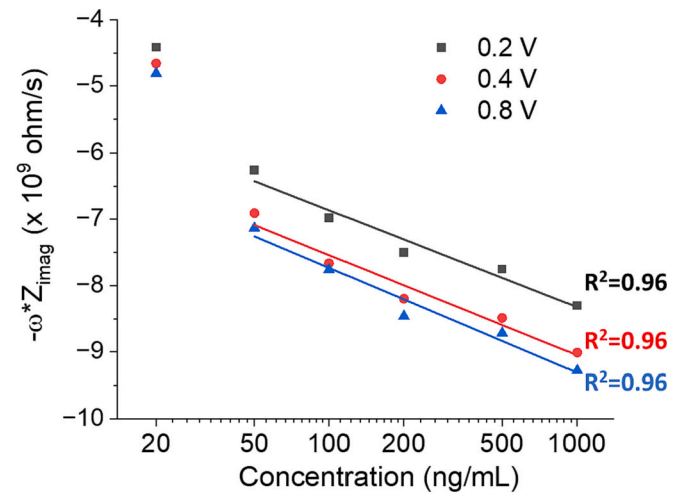


Fig. 5. Correlation between $-\omega^*Z_{\text{imag}}$ and concentration of NPY in aCSF at 0.2 V, 0.4 V, and 0.8 V, showing a linear correlation in all of them with $R^2 = 0.96$.

peak current of polypyrrole and NPY concentration as low as 20 ng/mL, showing a linear relationship between 50 ng/mL and 1000 ng/mL with $R^2 = 0.99$.

Because of the adsorption of NPY into the MIPPy electrodeposited on the surface of the carbon microelectrode, the capacitance of the electrode is also changed, as can be seen in the width of the CV. Therefore, we studied the capacitance using EIS from 10 Hz to 100 kHz to observe the changes produced by the adsorption of NPY on the surface. Fig. 4 shows the background-subtracted EIS obtained at 0.2 V (Fig. 4A), 0.4 V (Fig. 4B), and 0.8 V (Fig. 4C) vs Ag|AgCl. The data obtained at 0 ng/mL (as electrodeposited MIPPy) was subtracted to observe only the changes produced by the adsorption of NPY on the surface of the microelectrode.

Given the change in the width of the CV, we expected to observe a change in the capacitance of the electrode. This positively correlated to the data obtained with EIS. Fig. 4 shows $-\omega^*Z_{\text{imag}}$, which has been shown to be related to capacitance in carbon fiber microelectrodes with changes produced by specific surface adsorption. (Rivera-Serrano et al., 2018) The highest variation was seen at 100 kHz at each of the potentials measured, with little differences between the potentials.

Fig. 5 shows the correlation between $-\omega^*Z_{\text{imag}}$ and NPY concentrations measured with EIS. A similar relationship was found, as shown in CV measurements. The measurements were performed with concentrations as low as 20 ng/mL, with a linear relationship found between 50 and 1000 ng/mL with $R^2 = 0.96$. Similarly to the data obtained with CV, the result obtained at 20 ng/mL was outside the linear region. The sensor followed the typical activation range of concentrations, reaching a linear range between 50 ng/mL and 1000 ng/mL. The linear

relationship obtained at 0.8 V showed the highest slope compared to 0.2 V and 0.4 V although very similar between them. This is because the effect observed was the change in capacitance which was expected to be seen in the entire range of potentials.

4. Conclusions

In this conference paper, we were able to electrodeposit molecularly imprinted polypyrrole on carbon fiber microelectrodes of 7 μm in diameter and 150 μm in length. NPY was placed in the solution during the electrodeposition of polypyrrole, creating binding sites on the polymer structure. Characterization of polypyrrole showed the classic oxidation peaks at potentials higher than 0.6 V vs. Ag|AgCl. Using the oxidation peak at 0.73 V, we observed a decrease in current due to the NPY binding on the MIPpy surface with a linear relationship when plotting $i_{\text{ox}} \text{-Log } C_{\text{NPY}}$. A linear relationship was found in concentrations between 50 ng/mL and 1000 ng/mL. Because of the change in capacitance observed in the CV, we used EIS at 0.2 V, 0.4 V, and 0.8 V vs. Ag|AgCl and observed a correlation between the surface capacitance ($-\omega^* Z_{\text{imag}}$) and concentration of NPY at 100 kHz for each of the potentials between 50 ng/mL and 1000 ng/mL as well as with CV. While the testing of this sensor was limited to NPY₁₋₃₆, we were able to show that MIPpy electrodeposited on carbon fiber microelectrodes are a potential strategy for future measurement of NPY in the brain due to the high temporal and spatial resolution provided by carbon fiber microelectrodes in addition to the sensitivity to NPY of the MIPpy developed.

CRediT authorship contribution statement

Luis López: Writing – review & editing, Writing – original draft, Investigation, Formal analysis. **Kelly Lozano:** Investigation. **John Cruz:** Investigation. **Krystal Flores:** Investigation. **Lauren Fernández-Vega:** Writing – review & editing, Writing – original draft, Conceptualization. **Lisandro Cunci:** Writing – review & editing, Writing – original draft, Supervision, Methodology, Funding acquisition, Conceptualization.

Declaration of competing interest

The authors declare that they have no personal relationships or financial interests that could be perceived

Data availability

Data will be made available on request.

Acknowledgments

This work was supported by the National Institute of Mental Health under grant number 1R21 MH129037 and the National Science Foundation under award numbers 1827622 and 1849243. Students acknowledge the National Aeronautics and Space Administration Cooperative Agreement No. 80NSSC20M0052 (Puerto Rico Space Grant Consortium) and an Institutional Development Award (IDeA) from the National Institute of General Medical Sciences under grant number P20 GM103475-19 of the National Institutes of Health. This content is only the responsibility of the authors. It does not necessarily represent the official views of the National Institutes of Health, the National Science Foundation, or the National Aeronautics and Space Administration.

Appendix A. Supplementary data

Supplementary data to this article can be found online at <https://doi.org/10.1016/j.npep.2024.102413>.

References

Ayankojo, A.G., Boroznjak, R., Reut, J., Öpik, A., Syritski, V., 2022. Molecularly imprinted polymer based electrochemical sensor for quantitative detection of SARS-CoV-2 spike protein. *Sensors Actuators B Chem.* 353, 131160. <https://doi.org/10.1016/j.snb.2021.131160>.

Bath, B.D., Michael, D.J., Trafton, B.J., Joseph, J.D., Runnels, P.L., Wightman, R.M., 2000. Subsecond adsorption and desorption of dopamine at carbon-fiber microelectrodes. *Anal. Chem.* 72, 5994–6002. <https://doi.org/10.1021/ac000849y>.

Churcher, N.K.M., Upasham, S., Rice, P., Greyling, C.F., Prasad, S., 2022. Sweat based-multiplexed detection of NPY-cortisol for disease diagnostics and stress management. *Electroanalysis* 34, 375–386. <https://doi.org/10.1002/elan.202100083>.

Crespi, F., 2011. Influence of neuropeptide Y and antidepressants upon cerebral monoamines involved in depression: an *in vivo* electrochemical study. *Brain Res.* 1407, 27–37. <https://doi.org/10.1016/j.brainres.2011.05.033>.

Deškanić, A., Stevanović, J., Stevanović, R., Nikolić, B.Ž., Jovanović, V.M., 2001. Glassy carbon electrodes. *Carbon N Y* 39, 1195–1205. [https://doi.org/10.1016/S0008-6223\(00\)00228-1](https://doi.org/10.1016/S0008-6223(00)00228-1).

Duvall, L.B., Ramos-Espíritu, L., Barsoum, K.E., Glickman, J.F., Vossshall, L.B., 2019. Small-molecule agonists of ae Aegypti neuropeptide Y receptor block mosquito biting. *Cell* 176, 687–701.e5. <https://doi.org/10.1016/j.cell.2018.12.004>.

Eugster, P.J., Bourdillon, N., Vocat, C., Wuerzner, G., Nguyen, T., Millet, G.P., Grouzmann, E., 2022. Kinetics of neuropeptide Y, catecholamines, and physiological responses during moderate and heavy intensity exercises. *Neuropeptides* 92, 102232. <https://doi.org/10.1016/j.npep.2022.102232>.

Feier, B., Blidar, A., Pusta, A., Carciu, P., Cristea, C., 2019. Electrochemical sensor based on molecularly imprinted polymer for the detection of Cefalexin. *Biosensors (Basel)* 9, 31. <https://doi.org/10.3390/bios9010031>.

Gilpin, N.W., 2012. Neuropeptide Y (NPY) in the extended amygdala is recruited during the transition to alcohol dependence. *Neuropeptides* 46, 253–259. <https://doi.org/10.1016/j.npep.2012.08.001>.

Göttsche, C.R., Woldbye, D.P.D., 2016. The role of NPY in learning and memory. *Neuropeptides* 55, 79–89. <https://doi.org/10.1016/j.npep.2015.09.010>.

Kalra, S.P., Sahu, A., Kalra, P.S., Crowley, W.R., 1990. Hypothalamic neuropeptide Y: a circuit in the regulation of gonadotropin secretion and feeding behavior. *Ann. N. Y. Acad. Sci.* 611, 273–283. <https://doi.org/10.1111/j.1749-6632.1990.tb48938.x>.

Kim, S., Jang, L.K., Park, H.S., Lee, J.Y., 2016. Electrochemical deposition of conductive and adhesive polypyrrole-dopamine films. *Sci. Rep.* 6 <https://doi.org/10.1038/srep30475>.

Langley, D.B., Schofield, P., Jackson, J., Herzog, H., Christ, D., 2022. Crystal structures of human neuropeptide Y (NPY) and peptide YY (PYY). *Neuropeptides* 92, 102231. <https://doi.org/10.1016/j.npep.2022.102231>.

López, L., Hernández, N., Reyes Morales, J., Cruz, J., Flores, K., González-Amoretti, J., Rivera, V., Cunci, L., 2021. Measurement of neuropeptide Y using aptamer-modified microelectrodes by electrochemical impedance spectroscopy. *Anal. Chem.* 93, 973–980. <https://doi.org/10.1021/acs.analchem.0c03719>.

Lugo-Morales, L.Z., Loziuk, P.L., Corder, A.K., Toups, J.V., Roberts, J.G., McCaffrey, K.A., Sombers, L.A., 2013. Enzyme-modified carbon-fiber microelectrode for the quantification of dynamic fluctuations of nonelectroactive Analytes using fast-scan cyclic voltammetry. *Anal. Chem.* 85, 8780–8786. <https://doi.org/10.1021/ac4017852>.

Mintah Churcher, N.K., Upasham, S., Rice, P., Bhadsavle, S., Prasad, S., 2020. Development of a flexible, sweat-based neuropeptide Y detection platform. *RSC Adv.* 10, 23173–23186. <https://doi.org/10.1039/D0RA03729J>.

Morosawa, S., Iritani, S., Fujishiro, H., Sekiguchi, H., Torii, Y., Habuchi, C., Kuroda, K., Kaibuchi, K., Ozaki, N., 2017. Neuropeptide Y neuronal network dysfunction in the frontal lobe of a genetic mouse model of schizophrenia. *Neuropeptides* 62, 27–35. <https://doi.org/10.1016/j.npep.2016.12.010>.

Ping, Z., Junjie, L., Yunchun, L., 2022. Optimization of the electrodeposition process of a polypyrrole/multi-walled carbon nanotube fiber electrode for a flexible supercapacitor. *RSC Adv.* 12, 18134–18143. <https://doi.org/10.1039/D2RA02430F>.

Rivera-Serrano, N., Pagan, M., Colón-Rodríguez, J., Fuster, C., Vélez, R., Almodovar-Faria, J., Jiménez-Rivera, C., Cunci, L., 2018. Static and dynamic measurement of dopamine adsorption in carbon fiber microelectrodes using electrochemical impedance spectroscopy. *Anal. Chem.* 90, 2293–2301. <https://doi.org/10.1021/acs.analchem.7b04692>.

Rosas-Laverde, N.M.A., Pruna, A.I., Busquets-Mataix, D., 2020. Graphene oxide-Polypyrrole coating for functional ceramics. *Nanomaterials* 10, 1188. <https://doi.org/10.3390/nano10061188>.

Sajdyk, T.J., 2005. Neuropeptide Y receptors as therapeutic targets in anxiety and depression. *Drug Dev. Res.* 65, 301–308. <https://doi.org/10.1002/ddr.20031>.

Seibold, J.M., Abeykoon, S.W., Ross, A.E., White, R.J., 2023. Development of an electrochemical, aptamer-based sensor for dynamic detection of neuropeptide Y. *ACS Sens.* <https://doi.org/10.1021/acssensors.3c00855>.

Sharma, P.K., Gupta, G., Singh, V.V., Tripathi, B.K., Pandey, P., Boopathi, M., Singh, B., Vijayaraghavan, R., 2010. Synthesis and characterization of polypyrrole by cyclic voltammetry at different scan rate and its use in electrochemical reduction of the simulant of nerve agents. *Synth. Met.* 160, 2631–2637. <https://doi.org/10.1016/j.synthmet.2010.10.016>.

Singh, A., Sharma, A., Ahmed, A., Sundramoorthy, A.K., Furukawa, H., Arya, S., Khosla, A., 2021. Recent advances in electrochemical biosensors: applications, challenges, and future scope. *Biosensors (Basel)* 11, 336. <https://doi.org/10.3390/bios11090336>.

Sun, J., Wang, G., Zhang, H., Zhang, B., Hu, C., 2021. Facile fabrication of a conductive polypyrrole membrane for anti-fouling enhancement by electrical repulsion and in

situ oxidation. *Chemosphere* 270, 129416. <https://doi.org/10.1016/j.chemosphere.2020.129416>.

Tasan, R.O., Verma, D., Wood, J., Lach, G., Hörmer, B., de Lima, T.C.M., Herzog, H., Sperk, G., 2016. The role of neuropeptide Y in fear conditioning and extinction. *Neuropeptides* 55, 111–126. <https://doi.org/10.1016/j.npep.2015.09.007>.

Tilan, J., Kitlinska, J., 2016. Neuropeptide Y (NPY) in tumor growth and progression: lessons learned from pediatric oncology. *Neuropeptides* 55, 55–66. <https://doi.org/10.1016/j.npep.2015.10.005>.

Wagner, L., Kaestner, F., Wolf, R., Stiller, H., Heiser, U., Manhart, S., Hoffmann, T., Rahfeld, J.-U., Demuth, H.-U., Rothermundt, M., von Hörsten, S., 2016. Identifying neuropeptide Y (NPY) as the main stress-related substrate of dipeptidyl peptidase 4 (DPP4) in blood circulation. *Neuropeptides* 57, 21–34. <https://doi.org/10.1016/j.npep.2016.02.007>.

Yücebaş, B.B., Yaman, Y.T., Bolat, G., Özgür, E., Uzun, L., Abaci, S., 2020. Molecular imprinted polymer based electrochemical sensor for selective detection of paraben. *Sensors Actuators B Chem.* 305, 127368 <https://doi.org/10.1016/j.snb.2019.127368>.

Zhang, B., Nagle, A.R., Wallace, G.G., Hanks, T.W., Molino, P.J., 2015. Functionalised inherently conducting polymers as low biofouling materials. *Biofouling* 31, 493–502. <https://doi.org/10.1080/08927014.2015.1065487>.